Invited Paper

Novel RF MEMS Switches

S. Lucyszyn [1], S. Pranonsatit [2], J. Y. Choi [1], R. W. Moseley [3], E. M. Yeatman [1,3] and A. S. Holmes [1,3]
[1] Optical and Semiconductor Devices Group, Department of Electrical and Electronic Engineering
Imperial College London, Exhibition Road, London, SW7 2AZ, United Kingdom
[2] Department of Electrical Engineering,
Kasetsart University, Bangkok, Thailand
[3] Microsaic Systems Ltd, United Kingdom

***Abstract*—This paper reviews three novel RF MEMS ohmic contact switches, each being designed for specific applications. All three were developed at Imperial College London. The first is a packaged single-pole double throw (SPDT) version intended for space applications, operating from DC to 6 GHz; the second is a single-pole single throw (SPST) switch for high power applications in the 40 to 60 GHz band; and the third is a single-pole eight throw (SP8T) switch for signal routing applications, operating from DC to 20 GHz. The design, and measurements for all three unique solutions will be briefly summarized.**

Keywords-radio frequency; microelectromechanical systems; RF MEMS; switch; space; power; SPDT; SPST; SP8T

I. INTRODUCTION

RF microelectromechanical systems (RF MEMS) technology offers the potential for realizing very high-performance components [1-2]. This technology should not be confused with non-moving micromechanical structures [3-4]. By far the most important RF MEMS component is the switch. This is because RF MEMS switches have demonstrated orders of magnitude improvement in performance figure-of-merit over conventional PIN diode and switching-FETs. The first RF MEMS papers started to appear more than a quarter of a century ago, with electrostatically actuated cantilever-type switches. At around that time very little was reported, but over the last decade many papers have been published employing various RF MEMS technologies.

As with many technologies, one design is not appropriate for all applications. In particular, with RF MEMS switches, there may be a very limited number of solutions for specific applications. This paper describes the solutions adopted by Imperial College London and collaborators, for three specific applications; a packaged DC-6 GHz SPDT for space applications, 40-60 GHz SPST switch for high power applications and DC-20 GHz SP8T switch for signal routing applications.

II. DESIGN CONCEPTS

A. DC-6 GHz SPDT Switch [5]

For applications in space, such as satellite-based communication modules, the MEMS advantages of reduced power consumption and improved performance are very attractive. However, reliability and lifetime are paramount, the mechanical loads devices must withstand are severe, and high voltage supplies are normally undesirable. For this reason we chose to investigate an alternative design approach, namely thermally-actuated latched devices.

The use of coplanar waveguide (CPW) transmission lines was also examined, because the functionality to be addressed was SPDT, i.e. a selector switch between one input and two outputs. This can easily be configured as two series switches on each branch, fed from a Y-junction. However, since the open line presents a stub loading to the selected path, this stub must be kept very short, unless a (narrow-band) resonant structure is used. Since broadband performance is required in this case, the SPDT switch must be compact. While the CPW approach provides low loss and ease of fabrication, the large dimensions and weak confinement of the lines make such a compact design difficult to achieve without excessive compromises in performance.

Thin film microstrip (TFMS) transmission line was chosen rather than CPW, as it gives a laterally compact waveguide with strong field confinement. This allows a modest gap to be used, while still retaining high isolation. It also provides low cross-talk between the two signal paths. Consequently a short stub distance could be used between the two required gaps for the SPDT architecture.

As a result of the switch requirements, and the related considerations as discussed above, thermal actuation was chosen. Thermal actuators can provide high forces at low voltages, and do not inherently generate strong electric fields. However, they consume substantial power when driven and so to achieve low average power, a mechanically latching solution was also incorporated.

Fig. 1 shows a photomicrograph of the switched region. The actuators are of the shape bimorph type with lateral movement. A portal frame mechanism was used, i.e. two flexures with fixed separation at the fixed and free ends. This allows translation of the free end with minimal rotation. Set actuators are used to translate a plunger to make a connection across a gap in the line. Latches hold the set actuators in place and thus maintain continuity of the corresponding signal path when the actuator power is cut. The latched operation also supports the required insensitivity to shock and vibration. One latch part is joined to the end of the set actuator, the other is joined to the substrate via yet another portal frame flexure.

1-4244-0749-4/07/$20.00 @2007 IEEE.

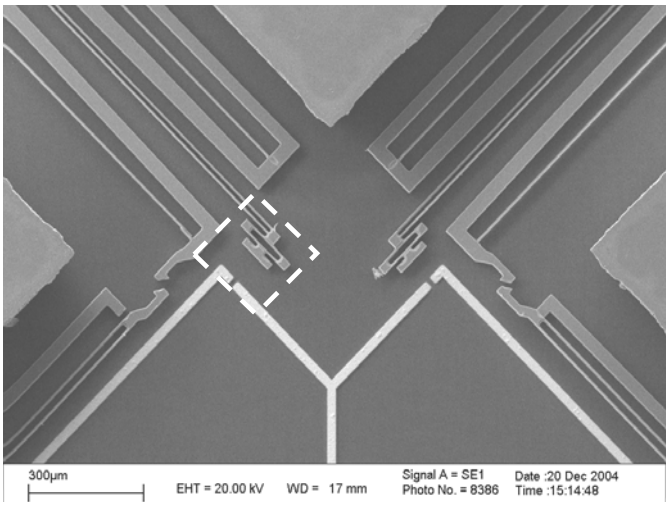

Figure 1. Electron micrograph of assembled SPDT switch for space applications [5] (plunger and transmission gap highlighted in dashed box)

The plungers are on flexible supports, so that they make contact before latching occurs and then deform with further actuation; this ensures the required mechanical force at the switch contacts in the ON state. These supporting flexures are inserted in rigid "wells" within the set actuators, so as to reduce the overall length of the structures, as this length can dominate the die size. Additional thermal actuators are incorporated to release the latches. The operating voltage for both set and release actuators is 3 V.

B. 40-60 GHz SPST Switch [6]

Traditional RF MEMS switches have inherent reliability issues associated with RF signal power handling (e.g. due to self-actuation, stiction, etc.). These problems can result from the membrane structure itself, which is very thin (typically 0.5 to 2 µm) and having very small gap separation distances (typically 1 to 5 µm) to an electrode. Because the power handling capacity varies with many variables associated with the switch architecture, there has been a lot of diverse efforts to improve RF signal power handling capacity. For example, the addition of a top electrode, above the membrane, to pull the membrane up; an array of a number of switching elements, to increase isolation and reduce current density; and an increase in the width and thickness of the membrane. However, these require an increase in the complexity of their design and fabrication, and are not fundamental solutions because a membrane-based architecture is still employed.

Using a previously established electrothermal hydraulic microactuator technology [7-11], a novel RF MEMS switch architecture is currently being developed that, in principle, can overcome many of the limitations associated with membrane-based architectures that employ electrostatic actuation.

The SPST switch can be seen in Fig. 2. It consists of two independent paraffin wax microactuators and out-of-plane silicon levers. Instead of membranes, silicon levers are designed with springs and latches that make an ohmic contact with the CPW's signal track. Paraffin wax microactuators control the silicon levers by means of a mechanical push and release mechanism. The simple latching mechanism can maintain both the OFF state and ON state, without continuous DC biasing of any microactuator.

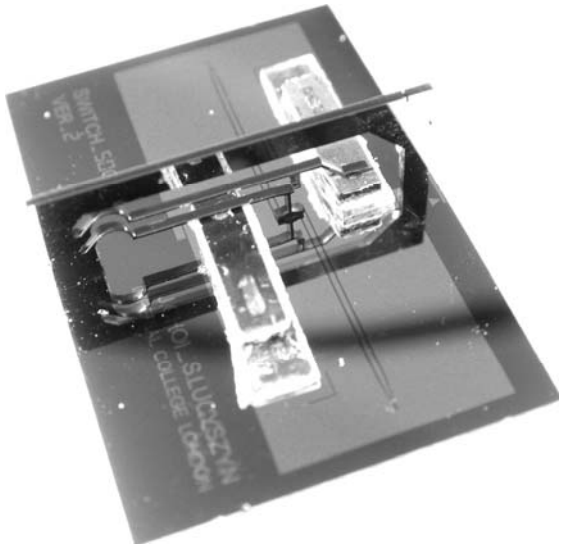

Figure 2. Photograph of assembled SPST switch for high power applications [6]

C. DC-20 GHz SP8T Switch [12-13]

Previous work on multi-throw RF MEMS switches has focused on arrays of single-pole single-throw (SPST) devices [14]. The only previous attempt to develop a truly rotary switch was by Larson and Hackett, who demonstrated capacitive RF switching in a radial-gap micromotor fabricated on GaAs [15]. In their design, the RF signal could travel only diagonally across the rotor, limiting the device to multiple SPST operation. Other issues such as poor repeatability were also highlighted by the authors.

We reported an alternative design of a rotary RF MEMS switch based on an axial-gap wobble motor. In this type of motor, the rotor sits at an oblique angle, with its centre raised and with a point on its periphery (the contact point) resting on the stator. By applying appropriate excitation voltages to drive electrodes on the stator, the rotor can be made to perform a precessional motion in which the contact point rotates continuously around the periphery of the device. This motion is similar to that of a coin flipped onto a table. The contact between rotor and stator is essentially one of rolling rather than sliding, and consequently motors of this type are expected to be less prone to wear than their salient pole counterparts. Also, the large overlap area between the drive electrodes and the rotor allows relatively large driving forces to be developed. To adapt the motor for RF switching, we have incorporated a number of CPW transmission lines as shown in Fig. 3. These include an input line (RF0), which connects to a bearing and axle at the centre of the stator, and eight output lines (RF1-RF8) that terminate at points just inside the circle inscribed by the contact point. Whenever the contact point lies on one of the output signal lines, an ohmic connection is made from that output line, through the rotor, to the bearing, and hence to the common input line. In this way the device functions as an SP8T rotary switch.

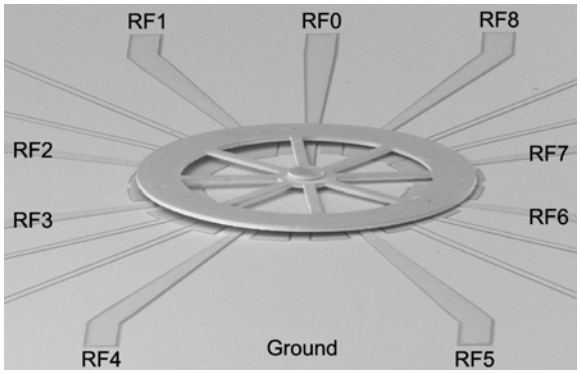

Figure 3. Electron micrograph of assembled SP8T switch (with cartwheel rotor) for signal routing applications [13]

III. Measured Performances

A. DC-6 GHz SPDT Switch [5]

TFMS is inevitably more lossy than CPW, because of its stronger field confinement (and hence high current density). A low propagation loss value of 0.1 dB/mm was achieved at 5 GHz, close to the modeled value. However, this loss factor still dominates the overall device losses, as shown in Fig. 4, owing to the long connection lengths in the current die and package design. A modification would substantially reduce line lengths to the die bond pads, and thus the insertion loss. The isolation was better than 50 dB across the 1 to 6 GHz range, which is well within the desired specification.

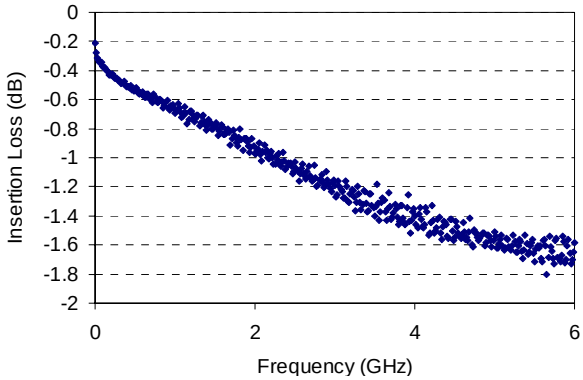

Figure 4. Measured die insertion loss for the SPDT switch

B. 40-60 GHz SPST Switch [6]

Preliminary measurements for the power switch could only be undertaken from DC to 8.5 GHz, and at small-signal power levels, as a suitable on-wafer V-band measurement system was not available to us at that time.

Fig. 5 shows the measured frequency responses. In the ON state, the measured minimum insertion loss and the maximum return loss were approximately 0.4 dB and 37 dB, respectively. The OFF-state isolation was higher than 23 dB. An applied bias of 12 V was required for each actuator, and the actuation time was 2-3 seconds.

Figure 5. Preliminary measurements of insertion loss for the SPST switch (well below the intended 40 to 60 GHz design frequency band)

C. DC-20 GHz SP8T Switch [12-13]

Initial tests were carried out in a 50 Ω test environment, where measured insertion loss varied from 0.4 dB at 1 GHz to 4 dB at 20 GHz (bottom graph in Fig. g). However, the basic rotary switches were not designed to operate at any particular frequency. Therefore, no impedance matching circuits were employed and, as a result, the switch exhibits a higher than normal level of insertion loss within a 50 Ω test environment, due to impedance mismatch reflection losses. To assess the significance of this effect, the insertion loss of a switch having a cartwheel rotor was renormalized to find the inherent levels of attenuation (i.e., without any mismatch losses). To this end, the identical measurement port impedances were optimized, at 20 different frequency points, to give simultaneous complex conjugate impedance matching (i.e. *Gmax*). This is equivalent to performing the function within some RF/microwave simulation software packages. In so doing, with the closed switch in the ON state, the insertion loss is minimized, due to the lack of any signal power reflections. The performance is shown in Fig. 6. It can be seen that the worst-case maximum insertion loss is now only 2.65 dB at 20 GHz.

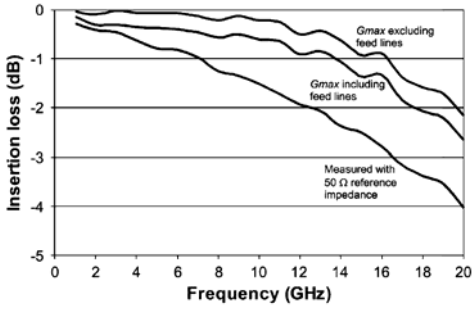

Figure 6. Measured insertion loss for the SP8T switch

It should be noted that these results include both the 1 mm long 50 Ω CPW feed lines. Much longer 50 Ω CPW test lines were included on the same wafer as the switches and subsequently accurately characterized. For example, at 20 GHz, an attenuation of 0.25 dB/mm was obtained from measurements of these test lines. Since both the input and output feed lines are approximately 1 mm long, the combined attenuation from these feed lines is 0.5 dB. Therefore, it can be concluded that the intrinsic loss of the switch having the cartwheel rotor is 2.16 dB at 20 GHz.

Fig. 6 also shows the performance with both the feed lines removed. It can be seen that the intrinsic losses are 0.02 dB at 3 GHz, 0.06 dB at 5 GHz, 0.22 dB at 10 GHz and 2.16 dB at 20 GHz. This can be compared with the measured performances of the side-drive rotary switch, presented by Larson and Hackett [15], which shows insertion losses of approximately 0.10 dB at 3 GHz, 0.10 dB at 5 GHz, 0.19 dB at 10 GHz, and 0.30 dB at 20 GHz. Our loss results can also be compared with the Tan *et al.* SP4T switch network, having a measured insertion loss of 0.15 dB at 3 GHz [14]. With our SP8T switch, the worst-case isolation was better than 30 dB from DC to 20 GHz.

From the accurate characterization of the 50 Ω CPW test lines, a model for the 1 mm long 50 Ω CPW feed lines was made. The intrinsic equivalent circuit model of an RF switch is commonly represented as a resistor in the ON state and a capacitor in the OFF state. Therefore, by embedding these crude lumped-elements between models for the feed lines, values for the ON-state resistance, R_{on}, and OFF-state capacitance, C_{off}, can be extracted using the measured data for insertion loss and isolation, respectively. The effective performance figure-of-merit can then be calculated from $f_c = (1/2\pi\ R_{on}\ C_{off})$ [1]. Using this parameter extraction technique, for an arbitrary switch position, the following values for $R_{on} = 18.6\ \Omega$ and $C_{off} = 0.8\ fF$ were found. The corresponding effective performance figure-of-merit is calculated to be $f_c = 10.7\ THz$.

IV. Conclusions

Around the world, there is a growing number of research and development groups working on a range of RF MEMS switch solutions for specific applications. While commercial successes have been reported in the US, as a result of vast amounts of investment (by DARPA, DOD, NASA and other government agencies), and are soon to be in Asia, Europe may soon join in [16]. As part of our own contribution to this effort, Imperial College London has identified three specific applications that require challenging and rather unorthodox solutions.

A SPDT packaged RF switch, with low voltage and low power operation, has been developed that is suitable for space and other applications. This demonstrated excellent RF performance between DC and 6 GHz. Ongoing research into high power RF MEMS switches for V-band and also L-band operation is continuing and preliminary results look very encouraging. Finally, a compact SP8T switch has been demonstrated for signal routing applications. This has already been successfully employed in 2-bit digital phase shifter demonstrators at 2, 5 and 10 GHz.

Acknowledgments

The authors would like to thank EADS-Astrium Ltd, UK, for their industrial support. Some of the work was also in association with the European Union's Network of Excellence in RF MEMS (AMICOM), under Framework 6, FP6-507352, and the UK Engineering and Physical Sciences Research Council (EPSRC), GR/N06366/01.

References

[1] S. Lucyszyn (Winner of IEE Premium Award), "Review of radio frequency microelectromechanical systems (RF MEMS) technology", IEE Proceedings – Science, Measurement and Technology, vol. 151, no. 2., pp. 93-103, Mar. 2004

[2] S. Lucyszyn (Invited Keynote Paper), "RF MEMS - an introduction", IEEE Workshop on MEMS for RF and Optoelectronics Applications, part of the international Wireless Design Conference, London, pp. 3-26, May 2002

[3] G. W. Dahlmann, E. M. Yeatman, P. R. Young, I. D. Robertson and S. Lucyszyn, "Fabrication, RF characteristics and mechanical stability of self-assembled 3D microwave inductors", Sensors and Actuators A-Physical, Elsevier Science, vol. 97-98, pp. 215-220, Apr. 2002

[4] M. P. Larsson and S. Lucyszyn, "A micromachined separable RF connector fabricated using low-resistivity silicon" Journal of Micromechanics and Microengineering, Institute of Physics Publishing, vol. 16, pp. 2021-2033, Aug. 2006

[5] R. W. Moseeley, E. M. Yeatman. A. S. Holmes, R. R. A. Syms, A. P. Finlay and P. Boniface, "Laterally actuated, low voltage, 3-port RF MEMS switch", 19th IEEE International Conference on Micro Electro Mechanical Systems (MEMS 2006), Turkey, pp. 878-881, Jan. 2006

[6] J. Y. Choi, J. S. Lee and S. Lucyszyn, "Development of RF MEMS switches for high power applications", IEEE Mediterranean Microwave Symposium (MMS'2006), Genoa, Italy, pp. 293-296, Sep. 2006

[7] J. S. Lee and S. Lucyszyn, "A micromachined refreshable Braille cell", IEEE/ASME Journal of Microelectromechanical Systems, vol. 14, no. 4, pp. 673-682, Aug. 2005

[8] J. S. Lee and S. Lucyszyn (Invited Paper), "Novel flat screen Braille display technology for the blind and partially sighted", 3rd International Conference on Materials for Advanced Technologies 2005 (ICMAT 2005) and 9th International Conference on Advanced Materials (IUMRS-ICAM 2005), Symposium C (Biomedical Devices & Instrumentation), Technical Session 7 – Microfluidics, Singapore, Jul. 2005

[9] J. S. Lee and S. Lucyszyn (Invited Paper), "Bulk-micromachined hydraulic microactuator", 3rd International Conference on Materials for Advanced Technologies 2005 (ICMAT 2005) and 9th International Conference on Advanced Materials (IUMRS-ICAM 2005), Symposium F (Nano-Optics & Microsystems), Technical Session 7 – Actuator, Singapore, pp. 115-118, Jul. 2005

[10] J. S. Lee and S. Lucyszyn, "Thermal analysis for bulk-micromachined electrothermal hydraulic microactuators using a phase change material", Sensors and Actuators A: Physical, Elsevier, vol. 135, no. 2, pp. 731-739, Apr. 2007

[11] J. S. Lee and S. Lucyszyn, "Design and pressure analysis for bulk-micromachined electrothermal hydraulic microactuators using a PCM", Sensors and Actuators A: Physical, Elsevier, vol. 133, no. 2, pp. 294-300, Feb. 2007

[12] S. Pranonsatit, A. S. Holmes, I. D. Robertson and S. Lucyszyn, "Single-pole eight-throw RF MEMS rotary switch", IEEE/ASME Journal of Microelectromechanical Systems, vol. 15, no. 6, pp. 1735-1744, Dec. 2006

[13] S. Pranonsatit, G. Hong, A. S. Holmes and S. Lucyszyn, "Rotary RF MEMS switch based on the wobble motor principle", 19th IEEE International Conference on Micro Electro Mechanical Systems (MEMS 2006), Istanbul, Turkey, pp. 886-889, Jan. 2006

[14] G.-L. Tan, R. E. Mihailovich, J. B. Hacker, J. F. DeNatale, and G. M. Rebeiz, "Low- loss 2- and 4-bit TTD MEMS phase shifters based on SP4T switches," IEEE Trans. Microw. Theory Tech., vol. 51, no. 1, pt. 2, pp. 297–304, Jan. 2003

[15] L. E. Larson, R. H. Hackett, M. A. Melendes, and R. F. Lohr, "Micromachined microwave actuator (MIMAC) technology-a new tuning approach for microwave integrated circuits," in Proc. IEEE Microw. Millimeter-Wave Monolithic Circuits Symp. Dig., Boston, MA, Jun. 1991, pp. 27–30

[16] S. Pranonsatit and S. Lucyszyn (Invited Paper), "RF-MEMS activities in Europe", Microwave Workshops and Exhibition (MWE 2005) Digest, Yokohama, Japan, pp. 111-122, Nov. 2005